Journal of Materials Chemistry C

PAPER

View Article Online
View Journal | View Issue

Published on 24 September 2014. Downloaded by Michigan State University on 26/01/2016 23:56:33.

Cite this: J. Mater. Chem. C, 2015, 3, 370

A systematic study of the structure–property relationship of a series of nonlinear optical (NLO) julolidinyl-based chromophores with a thieno[3,2-*b*]thiophene moiety†

Airui Zhang,[ab] Hongyan Xiao,[a] Shengyu Cong,[ab] Maolin Zhang,[ab] Hua Zhang,[ab] Shuhui Bo,*[a] Qi Wang,[a] Zhen Zhen*[a] and Xinhou Liu[a]

Received 24th August 2014
Accepted 18th September 2014

DOI: 10.1039/c4tc01896f

www.rsc.org/MaterialsC

A series of nonlinear optical (NLO) chromophores **a–d** bearing thieno[3,2-*b*]thiophene (TT) as the conjugated bridge or the lateral moiety have been synthesized and investigated. These chromophores display the same julolidinyl-based electron donor, but different electron acceptors (*i.e.*, 2-dicyanomethylene-3-cyano-4-methyl-2,5-dihydrofuran, TCF, or malononitrile). The solvatochromic behavior, thermal stability and electrochemical properties were evaluated to study the structure–property relationships. The solvent dependence of dipole moment (μ), static polarizability (α), hyperpolarizability (β) and bond length alternation (BLA) of all chromophores was demonstrated by density functional theory (DFT) calculations. Upon using the D–A–π–A structure, the blue-shifted phenomenon and substantially enhanced microscopic NLO properties of chromophore **d** were obtained. The electrooptic coefficient (r_{33}) of chromophore **a** (94 pm V^{-1} at 1.31 μm) was four times higher than that of chromophore **b** (~20 pm V^{-1}), while the calculated hyperpolarizability (β) of chromophore **b** was five times larger with respect to chromophore **a**. All the results demonstrated that the TT unit is a highly efficient conjugated bridge, and it has some electronical and sterical effects on macroscopic electrooptic (EO) activity when it is used as the lateral moiety. Guidelines can be proposed for the design of a new series of guest–host polymers including julolidinyl-based chromophores with a TT moiety, which could be useful in organic EO device fabrication.

Introduction

Organic second-order nonlinear optical (NLO) chromophores have been of considerable interest in ultrafast electrooptic (EO) applications over the last few decades.[1,2] The designed NLO chromophores were required to simultaneously exhibit large hyperpolarizability (β), strong thermal and photochemical stability as well as good optical transparency for practical EO device applications.[3–5] To achieve better NLO properties, significant advances in the development of novel organic EO materials have been made through rational molecular design[6–13] to optimize the ground-state polarization of the push–pull type chromophores by fine tuning the combination of an electron donor (D), an electron acceptor (A) and a π-conjugated bridge (π-bridge).[14–19] The methods such as using twisted π-conjugated systems,[20–22] alkali-metal-doped effects,[23] non-covalent charge transfer effects[14] and attaching the halogen atom[24] to the chromophores were all demonstrated to largely increase the EO properties of the materials. Recently, NLO chromophores with julolidinyl groups as the stronger electron donor have been studied and showed more excellent EO properties than chromophores with the classical dialkylamine donor for EO device applications.[25–29] Among them, chromophores with a julolidinyl-based donor, a thiophene-based electron bridge and a strong acceptor (*i.e.*, 2-dicyanomethylene-3-cyano-4-methyl-2,5-dihydrofuran, TCF) have been developed previously by our group which exhibit appealing NLO properties and good stability.[30,31] However, the β values of these chromophores can still be improved. Thus, the potentially attractive microscopic NLO properties of the julolidinyl-based chromophores are desirable to develop. And the enhanced β values coupled with excellent chemical and thermal stabilities are needed for practical EO applications.

Considering the best charge transfer (CT) efficiency, a polyene-type structure was introduced as the π-bridge between the donor and the acceptor. However, chromophores with olefinic fragments always associated with poor thermal stability that restricted their practical applications to a large extent. Thus, the

[a]Key Laboratory of Photochemical Conversion and Optoelectronic Materials, Technique Institute of Physics and Chemistry, Chinese Academy of Sciences, Beijing, 100190, PR China. E-mail: zhenzhenipc@gmail.com

[b]University of Chinese Academy of Sciences, Beijing 100049, PR China

† Electronic supplementary information (ESI) available: Quantum mechanical calculations, ^{1}H and ^{13}C NMR spectra of compounds. See DOI: 10.1039/c4tc01896f

This journal is © The Royal Society of Chemistry 2015

Published on 24 September 2014. Downloaded by Michigan State University on 26/01/2016 23:56:33.

replacement of a polyene-type structure by heteroaromatic compounds with lower aromatization energies was a common alternative to provide a good balance between NLO activity and stability.[32,33,34] Five-membered heterocyclic rings have been successfully developed as highly efficient π-bridges for CT.[32] Among them, thiophene has been widely employed in the heterocycle-based π-bridge, and so do some more complex structures like fused rings.[35–41] The thieno[3,2-*b*]thiophene (TT) unit, because of its good electron transfer ability, was mostly introduced to provide optimized planarity and intramolecular charge transfer (ICT) stability for organic photovoltaic applications.[42,43,44] But thieno[3,2-*b*]thiophene (TT) as the fused ring based π-bridge was rarely used in the NLO chromophores. And the reported chromophores with the TT unit did not show satisfied NLO properties due to the relatively weak donor and acceptor.[45,46] Moreover, thus, chromophores with the stronger donor–acceptor and TT based bridge are expected to provide higher NLO responses and better thermal stability.[46–48] However, to the best of our knowledge, few julolidinyl-based chromophores with a TT unit were studied, and they were expected to have high microscopic and macroscopic NLO properties.

According to the two-level model,[49] chromophores with a large dipole moment (μ) and β value always accompanied by long wavelength absorption, leading to the so-called nonlinearity–transparency trade-off and resulting in a large optical loss for EO modulator applications.[26] Therefore, one crucial way to search for the blue-shifted chromophores without the loss of nonlinearities is combining the different types of conjugated bridges. This novel concept was proposed to overcome the nonlinearity–transparency trade-off, but only a few studies on this concept were reported in recent years.[50,51] Consequently, chromophore **d** with combined bridges was designed and synthesized by two successive microwave methods, which were studied by us previously. This new designed D–A–π–A structure chromophore finely demonstrated this novel concept. In summary, these chromophores were expected to have high NLO properties as well as high thermal stability and to overcome the nonlinearity–transparency trade-off.

In this work, we focus our attention on the synthesis and characterization of six new chromophores **a–f** (with a TT unit) (see Schemes 1 and 2) bearing different π-bridges and acceptors and a fixed julolidinyl donor. The solvatochromism behaviour and thermal stability of all chromophores were also discussed in detail. Moreover, DFT calculations were carried out to demonstrate the solvent dependence of the static polarizability (α), β, μ, electron density, bond length alternation (BLA) and the energy gap (ΔE).[26] Through the theoretical calculation, the β value of chromophores, which contained the julolidinyl-based donor, TCF acceptor and TT-based π-bridge, was much larger than that of chromophores with a thiophene-based π-bridge. In this system, chromophores **a–d** were designed for the first time to discuss the effect of the TT unit as the π-bridge or the lateral moiety on the molecular polarization level and NLO responses. Chromophores **e** and **f** were synthesized without a TT unit for comparison. Finally, the macroscopic EO activity (r_{33} value) of chromophores **a** and **b** was studied by doping them into the amorphous polycarbonate (APC). The r_{33} values of poled film **a**/APC (94 pm V^{-1} at 1.31 μm) were almost four times larger with respect to **b**/APC (~20 pm V^{-1} at 1.31 μm).[52] The experimental measurements and theoretical calculations described herein helped us to recognize the electronic and geometric structures of these chromophores.

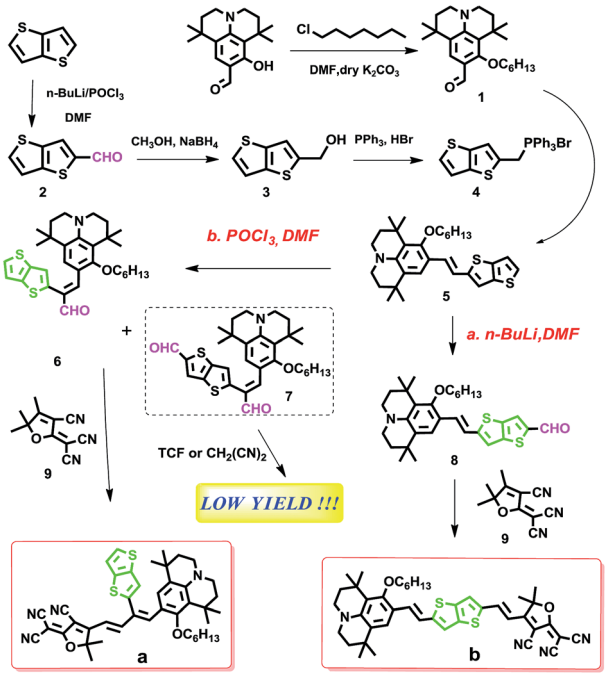

Scheme 1 Synthesis scheme for chromophores **a** and **b**.

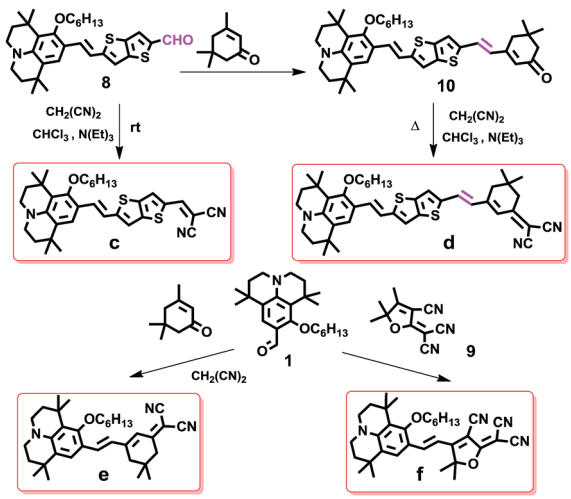

Scheme 2 Synthesis of chromophores **c**, **d**, **e** and **f**.

Experimental section

General methods

All reagents were purchased from commercial sources and were used as received unless otherwise specified. Solvents such as *N*,*N*-dimethylformamide (DMF) and tetrahydrofuran (THF)

Published on 24 September 2014. Downloaded by Michigan State University on 26/01/2016 23:56:33.

were freshly treated and distilled over calcium hydride and sodium, respectively, and stored under nitrogen prior to use. Phosphorus oxychloride ($POCl_3$) was distilled before use. The dielectric constants of six different solvents are 1,4-dixoane: 2.25, toluene: 2.38, chloroform: 4.81, dichloromethane: 8.93, acetone: 20.7, and acetonitrile: 37.5, respectively. The thieno [3,2-*b*]thiophene electron bridge and the 2-dicyanomethylen-3-cyano-4,5,5-trimethyl-2,5-dihydrofuran (TCF) acceptor were prepared according to the literature procedures,[53,54] respectively. UV-Vis-NIR spectra were obtained using a HITACHI U-2001 spectrometer. The TGA curve was recorded with a TA-instrument Q50 analyzer at a heating rate of 10 °C min^{-1} under a nitrogen atmosphere. Differential scanning calorimetry (DSC) measurements were performed on a TA5000, 2910MDSC with a heating rate of 10 °C min^{-1} under the protection of nitrogen. The MS spectra were obtained on a MALDI-TOF (Matrix Assisted Laser Desorption/Ionization of Flight) on a BIFLEXIII (Broker Inc.) spectrometer and on an EI (Electron Impact Source) with an ApexIII (7.0 tesla) FTICR mass spectrometer (Bruker). Cyclic voltammetry (CV) experiments were performed on a Princeton Applied Research Model 283 Potentiostat/Galvanostat. A three-electrode-system is used for the measurement and bulk electrolysis, with a 3 mm glass carbon working electrode, a platinum sheet counter electrode, and a non-aqueous $Ag/AgNO_3$ reference electrode for an organic solution reference electrode for aqueous solution. The electrolyte solution (0.1 M of *n*-Bu_4NPF_6 in CH_3CN for organic solution) was degassed by bubbling with argon for 40 min before measurement. The working electrode was polished with 0.05 μm alumina paste and sonicated for 15 min before use. ^1H NMR and ^{13}C NMR spectra were recorded on an AVANCE 400 (Bruker) spectrometer (400 MHz) using tetramethylsilane (TMS; $\delta = 0$ ppm) as the internal standard, respectively.

The DFT quantum chemical methods using the Gaussian 09 (ref. 58) software package in the gas phase and six different[60] solvents were carried out at the B3LYP/6-31G level. Geometry structures of each chromophore were optimized and resulted in a three dimensional D–π–A arrangement. The calculated parameters include electron density, μ, α, β, BLA and ΔE.

Electric field poling and EO property measurements

To study the poling and EO activity derived from the chromophores, guest–host polymers were generated by formulating chromophores **a** (20 wt%) and **b** (10 wt%) into amorphous polycarbonate (APC) using dibromomethane (CH_2Br_2) as the solvent. The resulting solutions were filtered through a 0.2 μm PTFE filter, and then spin-coated onto indium tin oxide (ITO) glass substrates (from thin film devices). Films of doped EO polymers were baked in a vacuum oven overnight to ensure the removal of the residual solvent. Corona poling was used to pole the films. The poling temperature was 135 °C for **a**/APC and 145 °C for **b**/APC. Then, a thin layer of aluminium (50–100 nm) was sputtered onto the films as the top electrode. The r_{33} values were measured by the Teng–Man simple reflection technique at the wavelength of 1.31 μm using a carefully selected thin ITO electrode with low reflectivity and good transparency in order to minimize the contribution from multiple reflections.[55]

General procedure for synthesis of compound 1. Under a N_2 atmosphere to a solution of 8-hydroxy-1,1,7,7-tetramethyl-formyljulolidine (2.73 g, 10 mmol) in anhydrous DMF were added 1-chloroheptane (2.02 g, 15 mmol) and K_2CO_3 (2.08 g, 15 mmol). The mixture was irradiated under microwaves (140 °C) for 35 min and then poured into water until it was cooled to ambient temperature. The resulting solutions were filtered and then extracted with ethyl acetate. The combined organic extracts were washed with brine and then dried over $MgSO_4$ and filtered. After the removal of the solvent, the residue was purified by column chromatography using petroleum ether and ethyl acetate (40 : 1, v/v) as an eluent to give the product as an yellow solid (2.96 g, yield: 83%). ^1H NMR (400 MHz, $CDCl_3$, δ ppm) 9.96 (s, 1H), 7.59 (s, 1H), 3.96 (t, $J = 6.9$ Hz, 2H), 3.29 (t, 2H), 3.23 (t, 2H), 1.93–1.82 (m, 2H), 1.76–1.66 (m, 4H), 1.46 (dd, $J = 8.6$, 4.1 Hz, 2H), 1.43 (s, 6H), 1.38–1.31 (m, 4H), 1.26 (s, 6H), 0.91 (t, $J =$ 7.0 Hz, 3H). ^{13}C NMR (101 MHz, $CDCl_3$, ppm) δ 187.75, 162.12, 148.20, 126.06, 125.29, 120.71, 117.26, 78.88, 47.46, 46.82, 39.41, 35.70, 32.44, 32.04, 31.74, 30.25, 30.01, 29.73, 25.63, 22.56, 14.01. MALDI-TOF-MS (*m*/*z*): calcd: 358.0; found: 359.2.

General procedure for synthesis of compound 2. A solution of thieno[3,2-*b*]thiophene (1 g, 7.13 mmol) in dry THF (30 mL) was cooled to −78 °C and was maintained at this temperature under a N_2 atmosphere during the dropwise addition of *n*-BuLi in hexane (2.5 M, 14.26 mmol). After the mixture was stirred at −78 °C for 1 h, it was warmed to −10 °C and held for 30 min. The solution was cooled back to −78 °C again, and kept at this temperature during the dropwise addition of dry DMF (10 mL). The reaction mixture was warmed to ambient temperature, and then quenched by adding 10 mL of water. The residue was extracted with ethyl acetate (3 × 50 mL). The combined organic layer was washed sequentially with brine and DI water, and then dried over $MgSO_4$, filtered, concentrated and purified by flash chromatography on silica gel using petroleum ether and ethyl acetate (80 : 3, v/v) to give compound **2** as an orange solid (1.02 g, 85%). ^1H NMR (400 MHz, $CDCl_3$, δ ppm) 9.96 (s, 1H), 7.93 (s, 1H), 7.69 (d, $J = 5.3$ Hz, 1H), 7.32 (d, $J = 5.3$ Hz, 1H). ^{13}C NMR (101 MHz, $CDCl_3$, δ ppm) 184.40, 146.56, 146.29, 140.05, 134.74, 129.92, 121.00. EI-MS (*m*/*z*): calcd: 167.9; found: 168.8.

General procedure for synthesis of compound 3. To a solution of compound **2** (1.68 g, 10 mmol) in methanol (20 mL) was added $NaBH_4$ (0.46 g, 12 mmol) in batches at 0 °C in an ice bath. After the temperature warmed up to room temperature and the solution became clear, diluted hydrochloric acid was added to neutralize the reaction and then kept stirring for 2 h. The solution was extracted with ethyl acetate; the combined organic extracts were washed with brine and dried over $MgSO_4$. After removal of the solvent, the residue was directly dried in the vacuum oven for the next step without flash chromatography. The product was a white solid (0.88 g, yield: 75%). ^1H NMR (400 MHz, acetone, δ ppm) 7.36 (d, $J = 5.2$ Hz, 1H), 7.19 (d, $J = 5.2$ Hz, 1H), 7.12 (s, 1H), 4.70 (d, $J = 5.9$ Hz, 2H), 1.91 (dt, $J = 4.3$, 2.2 Hz, 1H). ^{13}C NMR (101 MHz, acetone, δ ppm) 149.65, 139.62, 139.40, 127.49, 120.55, 117.40, 60.70. MALDI-TOF-MS (*m*/*z*): calcd: 170.0; found: 171.0.

 This journal is © The Royal Society of Chemistry 2015

Published on 24 September 2014. Downloaded by Michigan State University on 26/01/2016 23:56:33.

General procedure for synthesis of compound 4. Into about 20 mL of $CHCl_3$ was dissolved 0.5 g (2.94 mmol) of compound **3**. To this solution was added triphenylphosphine hydrobromide 1.14 g (3.32 mmol). The mixture was refluxed for 3 h. The solvent was evaporated under reduced pressure. The product was collected and washed with anhydrous ethyl ether, and used without further purification. The yield was 1.4 g (97% yield). The molecular formula without bromine was tested since the bromine is not observed. MALDI-TOF-MS (*m*/*z*): calcd: 414.1; found: 415.1.

General procedure for synthesis of compound 5. To a solution of compound **1** (1.91 g, 5.34 mmol) and compound **4** (2.64 g, 5.34 mmol) in dry THF (20 mL) was added NaH (2.40 g, 100 mmol). The solution was allowed to stir at room temperature for 24 h and then poured into water. The residue was extracted with ethyl acetate (3 × 50 mL). The combined organic layer was washed sequentially with brine and DI water, and then dried over $MgSO_4$, filtered, concentrated and purified by flash chromatography on silica gel using petroleum ether and ethyl acetate (100 : 1, v/v) to give compound **5** as an orange oil (1.32 g, 50%). ^{1}H NMR (400 MHz, $CDCl_3$, δ ppm) 7.18 (dd, J = 11.9, 6.7 Hz, 1H), 7.13–7.07 (m, 1H), 7.05 (s, 1H), 7.01 (s, 1H), 6.52 (s, 1H), 3.91 (t, J = 6.5 Hz, 1H), 3.86 (t, J = 6.5 Hz, 2H), 3.13–3.07 (m, 2H), 3.06–2.99 (m, 2H), 1.93–1.83 (m, 2H), 1.78–1.66 (m, 4H), 1.60–1.50 (m, 2H), 1.43 (s, 6H), 1.37 (m, 4H), 1.28 (s, 6H), 1.14 (s, 2H), 0.94–0.81 (m, 3H). ^{13}C NMR (101 MHz, $CDCl_3$, δ ppm) 154.99, 146.19, 141.89, 138.51, 135.71, 132.72, 132.52, 127.58, 127.41, 127.35, 125.46, 125.15, 124.76, 121.48, 118.47, 116.70, 115.24, 72.32, 46.33, 45.85, 39.39, 35.83, 31.66, 31.21, 30.85, 30.42, 29.34, 29.11, 24.95, 21.59, 12.92. MALDI-TOF-MS (*m*/*z*): calcd: 493.2; found: 494.2.

General procedure for synthesis of compounds 6 and 7. A solution of 20 mL DMF was cooled to 0 °C and was maintained at this temperature during the dropwise addition of freshly distilled phosphorus oxychloride ($POCl_3$, 0.64 g, 4.2 mmol). The solution was kept stirring for 2 h at 0 °C and this temperature was maintained during the dropwise addition of compound **5** in 10 mL DMF (1.0 g, 2 mmol). The solution was gradually warmed to room temperature and then heated to 90 °C for 3 h. The solution of Na_2CO_3 (10%, 150 mL) was added to quench the reaction which was then allowed to cool down to room temperature. The reaction mixture was extracted with ethyl acetate (3 × 50 mL), washed with brine, dried over $MgSO_4$ and filtered. After removal of the solvent under reduced pressure, the crude product was purified by flash chromatography on silica gel using petroleum ether and ethyl acetate (400 : 7, v/v) to give compound **6** as an orange solid (0.57 g, 55%) and to give compound **7** as an red solid (0.31 g, 28%). Compound **6**: ^{1}H NMR (400 MHz, $CDCl_3$ δ ppm) 9.63 (s, 1H), 7.62 (s, 1H), 7.32 (d, J = 5.2 Hz, 1H), 7.28 (s, 1H), 7.21 (d, J = 5.1 Hz, 1H), 7.04 (s, 1H), 3.94 (t, J = 6.7 Hz, 2H), 3.21–3.13 (m, 4H), 1.95–1.83 (m, 2H), 1.77–1.68 (m, 4H), 1.60–1.49 (m, 6H), 1.42 (s, 9H), 1.40–1.35 (m, 6H), 1.26 (s, 4H), 0.95–0.89 (m, 4H), 0.77 (s, 6H), 0.07 (s, 3H). ^{13}C NMR (101 MHz, $CDCl_3$, δ ppm) 191.27, 158.30, 148.56, 144.94, 139.24, 138.21, 136.49, 132.80, 132.61, 127.43, 126.06, 125.78, 124.65, 120.43, 118.90, 118.38, 113.06, 74.86, 46.35, 45.75, 38.62, 34.80, 31.50, 30.78, 30.71, 29.15, 28.91, 28.88, 24.84, 21.67, 13.03. MALDI-TOF-MS (*m*/*z*): calcd: 521.2; found: 522.2. Compound **7**: ^{1}H NMR (400 MHz, $CDCl_3$, δ ppm) 9.83 (s, 1H), 9.51 (s, 1H), 7.81 (s, 1H), 7.57 (s, 1H), 7.29 (s, 1H), 6.95 (s, 1H), 3.86 (t, 2H), 3.10 (t, 4H), 1.81 (s, 2H), 1.62 (m, 2H), 1.46 (m, 2H), 1.33 (s, 12H), 1.16 (m, 2H), 0.82 (m, 2H), 0.70 (s, 3H). ^{13}C NMR (101 MHz, $CDCl_3$, δ ppm) 190.31, 182.37, 158.55, 149.38, 145.46, 144.64, 144.01, 143.66, 138.95, 128.16, 126.04, 125.80, 124.78, 120.53, 119.33, 112.41, 75.33, 46.33, 45.74, 38.43, 34.53, 31.46, 30.74, 30.68, 29.12, 28.89, 28.78, 24.81, 21.56, 13.05. MALDI-TOF-MS (*m*/*z*): calcd: 549.2; found: 550.2.

General procedure for synthesis of compound 8. A solution of compound **5** (3.95 g, 8 mmol) in dry THF (50 mL) was cooled to −78 °C and was maintained at this temperature under a N_2 atmosphere during the dropwise addition of *n*-BuLi in hexane (2.5 M, 16 mmol). After the mixture was stirred at −78 °C for 1 h, it was warmed to −10 °C and held for 30 min. The solution was cooled back to −78 °C again, and kept at this temperature during the dropwise addition of dry DMF (12 mL). The reaction mixture was warmed to ambient temperature, and then quenched by adding 10 mL of water. The residue was extracted with ethyl acetate (3 × 70 mL). The combined organic layer was washed sequentially with brine and DI water, and then dried over $MgSO_4$, filtered, concentrated and purified by flash chromatography on silica gel using petroleum ether and ethyl acetate (60 : 1, v/v) to give compound **8** as an orange red solid (2.79 g, 67%). ^{1}H NMR (400 MHz, acetone, δ ppm) 9.95 (s, 1H), 8.16 (s, 1H), 7.45 (s, 1H), 7.38 (s, 1H), 7.28 (d, J = 16.1 Hz, 1H), 7.20 (d, J = 16.1 Hz, 1H), 3.84 (t, J = 6.6 Hz, 2H), 3.21 (t, 2H), 3.15 (t, 2H), 1.95–1.85 (m, 2H), 1.72 (t, 4H), 1.64–1.53 (m, 2H), 1.41 (s, 6H), 1.40–1.38 (m, 2H), 1.28 (s, 6H), 0.90 (s, 3H). ^{13}C NMR (101 MHz, acetone, δ ppm) 183.99, 157.63, 154.82, 147.42, 145.09, 137.61, 131.00, 129.33, 127.83, 123.78, 123.14, 118.02, 76.26, 48.05, 47.54, 41.26, 37.68, 33.56, 33.14, 32.81, 31.74, 31.07, 30.90, 26.99, 23.51, 14.53. MALDI-TOF-MS (*m*/*z*): calcd: 521.2; found: 522.2.

General procedure for synthesis of chromophore a. A mixture of compound **6** (2.61 g, 5 mmol) and acceptor **9** (1.09 g, 5.5 mmol) in 20 mL of ethanol was irradiated under microwaves (95 °C) for 15 min. The resulting mixture removed the solvent and purified through column chromatography using petroleum ether and ethyl acetate (6 : 1, v/v) as an eluent to give the product as dark green solids (2.63 g, yield: 75%). ^{1}H NMR (400 MHz, $CDCl_3$, δ ppm) 8.06 (d, J = 15.0 Hz, 1H), 7.51 (s, 1H), 7.44 (d, J = 5.2 Hz, 1H), 7.30 (d, J = 5.2 Hz, 1H), 7.13 (s, 1H), 6.60 (s, 1H), 6.09 (d, J = 15.0 Hz, 1H), 3.91 (t, J = 6.5 Hz, 2H), 3.24 (s, 4H), 2.00–1.87 (m, 2H), 1.78–1.66 (m, 4H), 1.61 (s, 9H), 1.55–1.47 (m, 2H), 1.40 (s, 12H), 1.26 (s, 2H), 1.04–0.86 (m, 4H), 0.64 (s, 6H), 0.07 (s, 3H). ^{13}C NMR (101 MHz, $CDCl_3$, δ ppm) 175.68, 172.06, 159.77, 153.00, 145.75, 139.43, 138.75, 138.03, 129.90, 127.82, 126.60, 126.30, 125.69, 124.96, 120.83, 119.06, 118.60, 114.79, 109.77, 95.57, 76.81, 64.54, 46.66, 46.02, 38.13, 31.44, 30.73, 30.55, 29.06, 28.52, 28.04, 25.40, 13.08. MALDI-TOF-MS (*m*/*z*): calcd: 702.2; found: 703.2.

General procedure for synthesis of chromophore b. A mixture of compound **8** (2.61 g, 5 mmol) and acceptor **9** (1.09 g, 5.5 mmol) was dissolved in ethanol (2 mL) and chloroform (18

Published on 24 September 2014. Downloaded by Michigan State University on 26/01/2016 23:56:33.

mL). To this solution was added 2 drops of triethylamine and then was refluxed at 90 °C for 3–5 h and monitored by TLC. After removal of the solvents, the residue was purified by column chromatography eluting with petroleum ether and ethyl acetate (10 : 1, v/v) to give a dark solid (2.45 g, 70%). ^{1}H NMR (400 MHz, $CDCl_3$, δ ppm) 7.91 (d, $J = 15.6$ Hz, 1H), 7.56 (s, 1H), 7.30 (s, 1H), 7.13 (s, 1H), 7.03 (d, $J = 15.9$ Hz, 1H), 6.58 (d, $J = 15.6$ Hz, 1H), 3.85 (t, $J = 6.7$ Hz, 2H), 3.24 (t, $J = 5.8$ Hz, 2H), 3.17 (t, 2H), 1.89 (m, 2H), 1.77 (m, 2H), 1.76 (s, 6H), 1.57 (m, 4H), 1.44 (s, 6H), 1.39 (s, 4H), 1.32 (s, 6H), 0.92 (t, $J = 7.0$ Hz, 3H). ^{13}C NMR (101 MHz, acetone, δ ppm) 182.97, 156.59, 153.78, 146.30, 144.30, 143.82, 136.63, 129.97, 128.29, 126.79, 122.74, 122.10, 117.11, 116.85, 75.22, 47.01, 46.50, 40.22, 36.64, 32.52, 32.10, 31.78, 30.71, 30.03, 29.87, 25.96, 22.48, 13.50. MALDI-TOF-MS (m/z): calcd: 702.2; found: 703.1.

General procedure for synthesis of chromophore c. A mixture of compound **8** (2.61 g, 5 mmol) and malononitrile (0.46 g, 7 mmol) was dissolved in 15 mL chloroform. To this solution was added 2 drops of triethylamine and was stirred at room temperature for 15 min. After removal of the solvents, the residue was purified by column chromatography eluting with petroleum ether and ethyl acetate (20 : 1, v/v) to give a dark solid (1.28 g, 45%). ^{1}H NMR (400 MHz, $CDCl_3$, δ ppm) 7.77 (d, $J = 19.1$ Hz, 2H), 7.27 (d, $J = 12.5$ Hz, 2H), 7.12 (s, 1H), 7.02 (d, $J = 15.9$ Hz, 1H), 3.84 (t, $J = 6.6$ Hz, 2H), 3.23 (t, 2H), 3.16 (t, 2H), 1.89 (m, 2H), 1.75 (m, 4H), 1.54 (m, 2H), 1.43 (s, 6H), 1.39 (s, 4H), 1.31 (s, 6H), 0.91 (s, 3H). ^{13}C NMR (101 MHz, $CDCl_3$, δ ppm) 175.56, 172.08, 159.75, 152.89, 145.51, 139.52, 138.84, 138.22, 129.84, 127.87, 126.58, 126.36, 125.76, 119.13, 118.61, 114.99, 111.89, 110.95, 110.88, 95.56, 76.79, 64.53, 46.73, 46.10, 38.31, 31.53, 30.75, 29.11, 28.62, 28.18, 25.38, 21.56, 13.02. MALDI-TOF-MS (m/z): calcd: 569.2; found: 570.1.

General procedure for synthesis of chromophore d. A mixture of compound **8** (2.61 g, 5 mmol), compound **4** (isophorone, 0.83 g, 6 mmol), and sodium ethoxide (7 mmol, 0.17 g sodium dissolved in 2 mL anhydrous ethanol) in 10 mL anhydrous ethanol was irradiated under microwaves (95 °C) for 30 min. Then the reaction was completed and cooled to room temperature. After the solvent was evaporated, the residue and malononitrile (0.46 g, 7 mmol) dissolved in 10 mL anhydrous ethanol were irradiated under microwaves (95 °C) for 20 min. Then the reaction was completed and cooled to room temperature. After the solvent was evaporated, the residue was purified by column chromatography using petroleum ether and ethyl acetate (10 : 1, v/v) as an eluent to give the product as black solids (2.41 g, yield: 70%). ^{1}H NMR (400 MHz, $CDCl_3$, δ ppm) 7.27 (s, 1H), 7.25 (s, 1H), 7.21 (d, $J = 15.7$ Hz, 1H), 7.13 (d, $J = 15.9$ Hz, 1H), 7.07 (s, 1H), 6.99 (d, $J = 15.9$ Hz, 1H), 6.80 (s, 1H), 6.72 (d, $J = 15.6$ Hz, 1H), 6.62 (s, 1H), 3.85 (t, $J = 6.7$ Hz, 2H), 3.19 (t, 2H), 3.12 (t, 2H), 2.59 (s, 2H), 2.43 (s, 2H), 1.92–1.82 (m, 2H), 1.75 (m, 4H), 1.55 (s, 4H), 1.43 (s, 6H), 1.38 (m, 4H), 1.31 (s, 6H), 1.08 (s, 6H), 0.91 (t, $J = 7.0$ Hz, 3H). ^{13}C NMR (101 MHz, $CDCl_3$, δ ppm) 170.32, 168.65, 159.71, 156.39, 153.50, 150.58, 142.52, 141.91, 137.56, 130.90, 130.71, 128.85, 127.41, 122.85, 122.60, 120.59, 116.50, 113.17, 113.07, 112.39, 78.28, 75.34, 47.48, 46.98, 45.69, 42.94, 42.64, 39.18, 36.70, 32.75, 32.35, 32.00, 31.91, 31.30, 30.28, 30.17, 29.70, 28.03, 27.81, 26.02, 25.28, 22.67, 14.08. MALDI-TOF-MS (m/z): calcd: 689.2; found: 689.8.

General procedure for synthesis of chromophore e. A mixture of compound **1** (1.79 g, 5 mmol), compound **4** (isophorone, 0.83 g, 6 mmol), and sodium ethoxide (7 mmol, 0.17 g sodium dissolved in 2 mL anhydrous ethanol) in 10 mL anhydrous ethanol was irradiated under microwaves (95 °C) for 30 min. Then the reaction finished and cooled to room temperature. After the solvent was evaporated, the residue and malononitrile (0.46 g, 7 mmol) dissolved in 10 mL anhydrous ethanol were irradiated under microwaves (95 °C) for 20 min. Then the reaction finished and cooled to room temperature. After the solvent was evaporated, the residue was purified by column chromatography using petroleum ether and ethyl acetate (80 : 3, v/v) as an eluent to give the product as dark purple solids (1.99 g, yield: 76%). ^{1}H NMR (400 MHz, $CDCl_3$, δ ppm) 7.35 (s, 1H), 7.29 (d, $J = 16.0$ Hz, 1H), 6.78 (d, $J = 15.7$ Hz, 1H), 6.77 (s, 1H), 3.79 (t, $J = 6.7$ Hz, 2H), 3.26 (t, 2H), 3.19 (t, 2H), 2.58 (s, 2H), 2.46 (s, 2H), 1.92–1.79 (m, 2H), 1.79–1.66 (m, 4H), 1.56–1.47 (m, 2H), 1.42 (s, 6H), 1.39–1.34 (m, 4H), 1.31 (s, 6H), 1.06 (s, 6H), 0.92 (t, 3H). ^{13}C NMR (101 MHz, $CDCl_3$, δ ppm) 169.07, 157.96, 156.09, 145.02, 134.84, 127.33, 123.48, 123.05, 121.03, 114.68, 113.97, 76.45, 47.62, 47.05, 43.09, 39.82, 39.50, 36.23, 32.36, 32.38, 32.09, 32.03, 30.87, 30.31, 30.09, 29.81, 28.21, 26.17, 22.76, 14.19. MALDI-TOF-MS (m/z): calcd: 525.4; found: 526.4.

General procedure for synthesis of chromophore f. A mixture of compound **1** (1.78 g, 5 mmol) and acceptor **9** (1.09 g, 5.5 mmol) in 20 mL of ethanol was irradiated under microwaves (95 °C) for 15 min. The resulting mixture removed the solvent and purified through column chromatography using petroleum ether and ethyl acetate (10 : 1, v/v) as an eluent to give the product as dark green solids (2.02 g, yield: 75%). ^{1}H NMR (400 MHz, $CDCl_3$, δ ppm) 7.73 (d, $J = 15.6$ Hz, 1H), 7.42 (s, 1H), 6.73 (d, $J = 15.8$ Hz, 1H), 3.79 (t, $J = 7.3$ Hz, 2H), 3.42 (t, $J = 6.2$ Hz, 2H), 3.35 (t, 2H), 1.97–1.87 (m, 2H), 1.76 (s, 6H), 1.75–1.72 (m, 2H), 1.43 (s, 6H), 1.34 (dd, $J = 7.3$, 3.4 Hz, 4H), 1.30 (s, 6H), 0.91 (t, 3H). ^{13}C NMR (101 MHz, $CDCl_3$, δ ppm) 174.07, 160.68, 149.17, 143.87, 130.91, 128.85, 128.32, 124.39, 122.44, 115.50, 113.35, 112.54, 111.90, 107.18, 96.06, 71.79, 65.55, 47.94, 47.28, 38.88, 35.12, 32.50, 32.09, 31.75, 29.72, 29.31, 27.12, 25.62, 22.57, 13.99. MALDI-TOF-MS (m/z): calcd: 538.3; found: 539.1.

Results and discussion

Chromophores **a** and **b** were synthesized as shown in Scheme 1. Compound **2** with one aldehyde group was obtained through two methods of the formylated reaction using *n*-butyllithium (*n*-BuLi) and DMF, and the Vilsmeier reaction with phosphorus oxychloride ($POCl_3$) and DMF. Both methods can introduce only one aldehyde group by one step approach with high yields (>90%), when *n*-BuLi, $POCl_3$ and DMF were in excess. Compound **2** was then reduced to alcohol **3** and transferred to Wittig salt **4**. Afterwards, compound **1** reacted with Wittig salt **4** following Wittig reaction to obtain compound **5**. Through a Vilsmeier reaction, the TT unit in compound **6** was also found as a dual-function structure and provided steric hindrance and electronic effects.[31] The formation of the unexpected compound

 This journal is © The Royal Society of Chemistry 2015

Published on 24 September 2014. Downloaded by Michigan State University on 26/01/2016 23:56:33.

7 with two aldehyde groups was resulted from the excess $POCl_3$ and DMF. Due to the slight electron-withdrawing properties of the aldehyde group, it was hard for compound 7 to condense with two acceptors simultaneously with considerable yield. Compound **8** was obtained by deprotonation of compound **5** with *n*-BuLi followed by reaction with DMF. Finally, compounds **6** and **8** were coupled with acceptor **9** to obtain target chromophores **a** and **b**, respectively.

To study the influence of acceptor strength and the combined bridge effect on the nonlinearity, chromophores **c** and **d** were designed and shown in Scheme 2. Noticeably, chromophore **d** was synthesized by two successive microwave (MW)-assisted condensation methods introduced by us previously, which demonstrated that MW-assisted heating was a highly efficient method in the synthesis of NLO chromophores. All the chromophores exhibited good solubility in common organic solvents, such as acetone, DMSO, CH_2Cl_2, DMF, $CHCl_3$, and THF. The structures of the compounds were characterized unambiguously by ^{1}H NMR, ^{13}C NMR and MALDI-TOF-MS.

Thermal stability

The thermal properties of chromophores **a–f** were evaluated by differential scanning calorimetry (DSC) and thermal gravimetric analysis (TGA) in nitrogen with the results shown and tabulated in Fig. 1 and Table 1. All chromophores except chromophore **b** displayed crystalline characteristics with a melting point (T_m). Obviously, chromophore **b** was obtained as a thermodynamically stable amorphous glass state solid showing a glass transition temperature (T_g) at around 125 °C. The amorphous state of chromophore **b** was mainly attributed to both the longer π-bridge and the stronger TCF acceptor, which disfavoured the close packing of molecules. The strong T_m peak of chromophore **d** showed that the combined bridge structure could promote chromophore molecule crystallization.

The TGA results did not follow the same trends as DSC results. Chromophore **e** showed the highest decomposition temperature (T_d), while chromophore **d** showed the lowest T_d, which might be due to the 'mismatched' combination of TT and isophorone units.[33] Chromophore **b** displayed higher T_d than **a**, suggesting that chromophores with a TT unit as the π-bridge can increase the thermal stability compared with the reported polyene-type chromophore (212 °C).[4] By comparison of chromophores **b** and **c**, it can be concluded that the TCF acceptor helped to increase the thermal stability, which was in agreement with T_g values. As a result, chromophores **a**, **b** and **e** displayed the sufficient thermal stabilities (T_d is higher than 200 °C) for applications in device fabrication.

Table 1 Thermal properties of chromophores **a–f**

Compd	T_g/T_m (°C)	T_d (°C)
a	205	238
b	125	276
c	217	174
d	75	130
e	166	296
f	203	164

UV-Vis-NIR spectroscopy

The solvatochromic behavior of chromophores is strongly influenced by the strength of the donor and acceptor in combination with the π-bridge. To reveal the solvent dependence effect of the π-bridge and acceptor on the electronic structures of chromophores **a–f**, the UV-Vis-NIR absorption spectra were recorded in six solvents with different dielectric constants (Fig. 2) and the corresponding optical absorption data are recorded in Table 2. All the chromophores showed intense low-energy ICT absorption bands except for chromophore **d**. Distinctively, chromophore **d** displayed a weak low-energy ICT absorption band and an intense and narrow high-energy ICT band, which was assigned to the π–π* transition of the aromatic moiety. It was presumed that the resonant

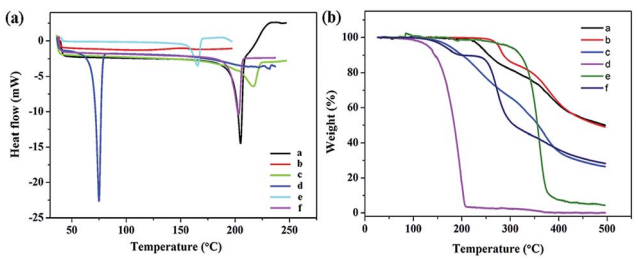

Fig. 1 The DSC and TGA curves of chromophores **a–f** with a heating rate of 10 °C min^{-1} in nitrogen.

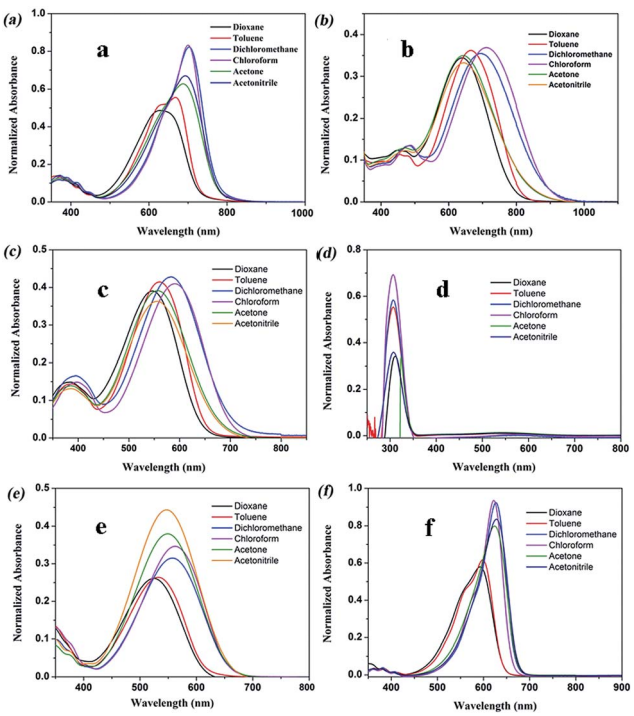

Fig. 2 Solvatochromic behavior of chromophores **a–f** recorded in six solvents (10^{-5} M) of varying dielectric constants at room temperature.

Published on 24 September 2014. Downloaded by Michigan State University on 26/01/2016 23:56:33.

Table 2 Summary of low-energy optical absorption data[a]

	Absorption λ_{max} (nm)						
Cmpd	DO	TL	CF	DC	AC	AN	$\Delta\lambda_{max}$
a	628	668	700	703	688	693	75
b	640	666	712	696	644	643	72
c	546	560	591	583	557	555	45
d	546	565	585	578	547	539	46
e	525	532	562	558	549	547	37
f	593	598	622	627	624	628	35

[a] DO: dixoane; TL: toluene; CF: $CHCl_3$; DC: CH_2Cl_2; AC: acetone; AN: acetonitrile.

structures of the combination of the TT unit and isophorone unit disfavored the ICT from the electron donor to the acceptor.[33] In combination with the poor thermal stability, we called this the 'mismatched' phenomenon. With the increase of solvent polarity, all the chromophores red-shifted initially, reaching the maximum value in chloroform or dichloromethane, and then, chromophores **a**, **e** and **f** exhibited the saturation behaviors. The cyanine-like characteristic (the neutral and charge-separated limiting resonance forms contributed equally to the ground state) band shape of them indicated that the two limiting resonance forms have approximately the same contribution to the ground state.[25] Chromophores **b** and **c** were polarized distinctly beyond the cyanine limit into the zwitterionic regime in acetone and acetonitrile solvents. While for chromophore **e**, a slight blue-shift was observed. Furthermore, chromophores **a** and **f** showed the relatively small fwhm (full width at half maximum) of the low-energy ICT absorption band and the most intensified absorbance in high polar solvents due to the short polyene π-bridge and the strong TCF acceptor.[26,56]

Comparison of chromophores **b** and **c** with different acceptors showed that the λ_{max} blue-shifted with the decrease of acceptor strength and the λ_{max} blue-shifted from chromophores **f** to **e**. This suggested that chromophores with a stronger acceptor were easier to polarize. As for the chromophore **d**, the λ_{max} decreased especially in highly polar solvents, demonstrating that chromophore **d** with the combination of the TT unit and isophorone unit as the π-bridge blue-shifted in comparison with its analogue (chromophore **c**) with a single type of π-bridge. The maximal wavelength difference ($\Delta\lambda_{max}$) of all chromophores in six different solvents is depicted in Table 3. Chromophores **a** and **b** showed larger $\Delta\lambda_{max}$ with respect to chromophores **c** and **d**, and chromophores **e** and **f** with shorter π-bridges showed smaller $\Delta\lambda_{max}$ values than others. It was suggested that chromophores **a** and **b** were the easiest to be polarized among all the chromophores.

Electrochemical properties and spectroscopic analysis for ΔE

The electrochemical behavior is closely related to the orbital structures of the highest occupied molecular orbital (HOMO) and the lowest unoccupied molecular orbital (LUMO) for the compounds. Thus, the oxidation and reduction potentials tested from electrochemical cyclic voltammetry (CV) measurements can provide important information for the HOMO–LUMO gap (ΔE). All the chromophores exhibited a single reversible or a quasi-reversible oxidative wave in positive energy and a single reversible reductive peak in negative energy (Fig. S1, ESI†). Table 2 shows that the HOMOs were similar for chromophores **b** and **c** because of the same donor part, while the LUMOs systematically lowered with an increase of the acceptor strength, leading to the decreased ΔE. Moreover, due to the increased length of the π-bridge, chromophore **b** showed the smallest ΔE (0.85 eV) and the chromophore **f** showed the largest ΔE (1.44 eV). The observed electrochemical behavior was in accord with the calculated orbital energy levels and ICT process of HOMO and LUMO for the chromophores studied in the following part.

As shown in Table 3, ΔE values of all the chromophores were also calculated through the UV-Vis-NIR absorption spectra by doping them into the APC polymer films. The ΔE values of spectral analysis and CV measurements followed the same trend, and the former were larger with respect to the latter. This can be attributed to the fact that the spectral results were tested in polymer films while the CV results were tested in acetonitrile solutions.

DFT calculations

First- and second-order polarizability. To profoundly understand the microscopic NLO properties of the designed chromophores, DFT calculations were performed at the B3LYP/6-31G level using the Gaussian 09 program package.[55,60] The calculated average static polarizability (α) can be obtained using eqn (1) (Table S1, ESI†). The total first hyperpolarizability (β_{tot}) of the designed chromophores (Table S2, ESI†) related to the individual tensor components can be obtained using eqn (2). They were calculated by the finite field method based on the optimized molecular geometries. β_i ($i = x$, y, and z) is defined using eqn (3)–(5) and μ can be obtained using eqn (6)

$$\alpha = (\alpha_{xx} + \alpha_{yy} + \alpha_{zz})/3 \quad (1)$$

$$\beta_{tot} = (\beta_x^2 + \beta_y^2 + \beta_z^2)^{1/2} \quad (2)$$

$$\beta_x = \beta_{xxx} + \beta_{xyy} + \beta_{xzz} \quad (3)$$

$$\beta_y = \beta_{yyy} + \beta_{yzz} + \beta_{yxx} \quad (4)$$

$$\beta_x = \beta_{zzz} + \beta_{zxx} + \beta_{zyy} \quad (5)$$

$$\mu = (\mu_x^2 + \mu_y^2 + \mu_z^2)^{1/2} \quad (6)$$

The α of chromophores **a–f** is shown in Fig. 3(a). It was found that chromophores with longer or similar length of conjugated bridges showed larger or similar α values. Moreover, the α values of chromophores in solvents were larger than that in the gas phase, and showed the increased tendency with the increase of the solvent permittivity. It was demonstrated that chromophore **b** with the longest conjugated bridge was the most

 This journal is © The Royal Society of Chemistry 2015

Published on 24 September 2014. Downloaded by Michigan State University on 26/01/2016 23:56:33.

Table 3 Measured and calculated parameters from the electrochemical and the absorption spectroscopic experiments

	Electrochemical analysis					Spectroscopic analysis	
Compd	E_{ox}[a], V	E_{red}[a], V	E_{HOMO}[b] (eV)	E_{LUMO}[b] (eV)	ΔE[c] (ev)	λ_{onset}[d], nm	ΔE[e] (eV)
a	0.21	−0.90	−4.60	−3.49	1.11	870	1.42
b	0.03	−0.82	−4.42	−3.57	0.85	948	1.31
c	0.01	−1.15	−4.40	−3.24	1.16	753	1.65
d	0.001	−1.13	−4.39	−3.26	1.13	766	1.62
e	0.06	−1.16	−4.45	−3.23	1.22	717	1.73
f	0.35	−1.09	−4.47	−3.30	1.44	715	1.73

[a] Potentials *vs.* Ag/Ag^+ in 0.1 M $TBAPF_6$/MeCN solution. [b] $E_{HOMO} = -e[4.39\ V + E_{ox}]$ and $E_{LUMO} = -e[4.39\ V + E_{red}]$. [c] $\Delta E = E_{HOMO} - E_{LUMO}$. [d] Estimated from the onset of the absorption at low concentration chromophores in solid films in APC. [e] $\Delta E = 1240/\lambda_{onset}$.

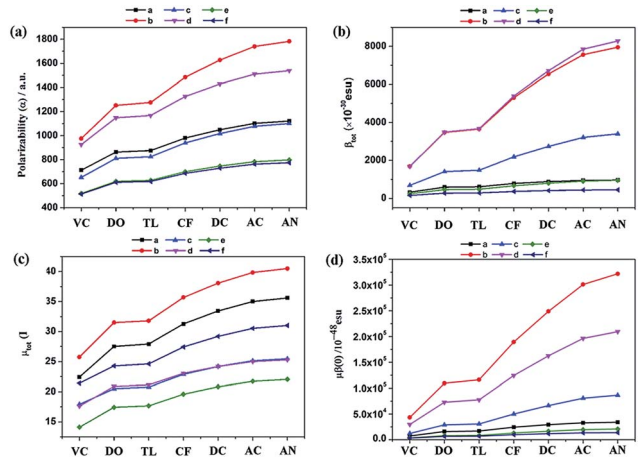

Fig. 3 The solvent dependence of (a) α, (b) β_{tot}, (c) μ, and (d) $\mu\beta$ was calculated in the gas phase and six solvents (Table S7–S10, ESI†). VC: vacuum.

vulnerable to the effects of solvent polarity of all the chromophores.

Fig. 3(b) shows the calculated β_{tot} (Table S4, ESI†) in the gas phase and solvents. Chromophores **b** and **d** gave a similar β_{tot} value, which was much larger than that of other chromophores. It was demonstrated that chromophores with longer π-bridges and stronger acceptors offered larger β_{tot}, and were consistent with the trend of the α value. In contrast, chromophore **a** showed a lower β_{tot} value than that of chromophore **c**. This was ascribed to the existence of the special lateral TT moiety that was used as the lateral moiety and could disperse three directional β_i ($i = x$, y, and z) tensors and tended to lower the β_{tot} value. All the chromophores showed a similar increasing trend of β_{tot} to a certain extent as a function of increasing solvent dielectric constant. The slopes were steep for chromophores **b** and **d**, and relatively smooth for chromophores **a**, **e**, and **f**, suggesting that chromophores with longer π-bridges showed larger β_{tot} values and bigger changes with the increase of dielectric constant. This followed the similar trend of the α value. Especially, chromophore **d** showed the largest calculated β_{tot} value among all six chromophores, and the blue-shifted phenomenon in UV-Vis-NIR spectra was also found for chromophore **d** that was mentioned previously. Thus, it was demonstrated that the combination of different π-bridges could lead to overcoming the nonlinearity–transparency trade-off.

The μ of chromophores **a–f** is displayed in Fig. 3(c) and tabulated (Table S3, ESI†). Chromophore **b** showed the largest μ due to the strong acceptor and good planarity. Chromophore **a** had larger μ with respect to chromophore **f** due to its longer π-bridge. Though chromophore **d** had much larger β_{tot} than that of chromophore **c**, it showed almost the same μ as **c**. It can be explained that the combined π-bridge could not only increase β_{tot}, but also decrease μ.

Because of the largest μ and β_{tot} values, chromophore **b** showed the largest $\mu\beta$ value (Fig. 3(d), Table S4, ESI†), which had great potential for NLO applications. Chromophore **d** showed a lower $\mu\beta_{tot}$ value than **b** due to the lower μ. Chromophores **a**, **e**, and **f** showed similar $\mu\beta_{tot}$ values due to the similar β_{tot}. Above all, the calculation results could provide us useful parameters for reference in designing the novel chromophores and predict their NLO properties.

Calculated Mulliken charges. Mulliken charge analysis was reported as a useful method to understand the ground state electronic structure and estimate the molecular polarization.[45] Therefore, the Mulliken charges on various molecular domains for the studied chromophores were calculated in the gas phase and are shown in Fig. 4.

Comparison of chromophores **a** and **b** showed that the TT moiety both lateral moiety and π-bridge exhibited electronegativity. And the negative charge located in the TT moiety as the lateral moiety is higher than that as the π-bridge due to the strong electron-withdrawing stability of the TCF acceptor. However, the charge in the TT unit for chromophore **c** was electropositive, resulting in the strong TCF electron acceptor tending to increase charge separation. In contrast, comparison of chromophores **c** and **d** with chromophores **e** and **f** showed that extending the conjugation length changed the electron properties of the TT unit from electropositive to electronegative and disfavored the charge separation. And chromophore **d** showed the approximate D–A–π–A structure. These phenomena revealed that the TT unit was regarded as an auxiliary acceptor in **d** and as an auxiliary donor in **c**. Thus, we speculated that the π-bridges favored to form the D–A–π–A structure, and it could favor to overcome the nonlinearity–transparency trade-off.

Published on 24 September 2014. Downloaded by Michigan State University on 26/01/2016 23:56:33.

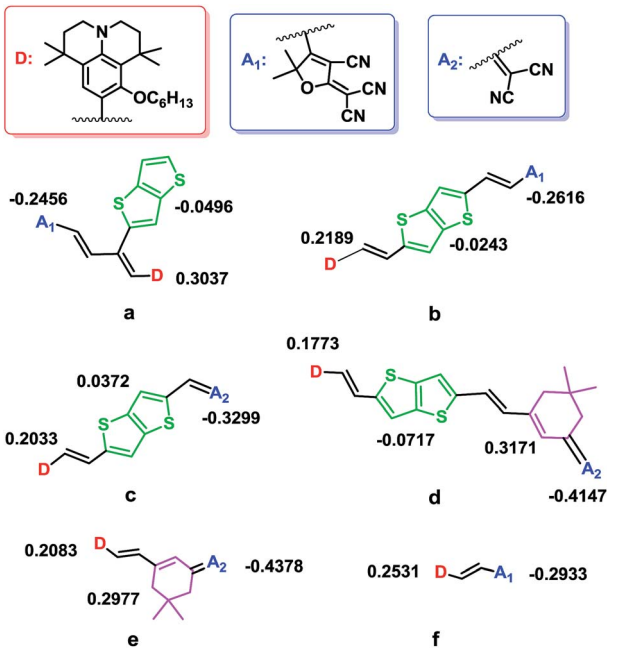

Fig. 4 Mulliken atomic charges on various molecular domains for six studied chromophores at the B3LYP/6-31G level. The moieties in color were considered for charge calculation.

Furthermore, the D–A–π–A structure chromophore could be used as a key part in dye-sensitized solar cells (DSSCs).[57]

Mulliken charges on various molecular domains for above chromophores were also calculated in six different solvents to study the solvent dependence of the ICT. For the donor and acceptor moieties, ICT of the six chromophores increased with the increase of the dielectric constant of solvents. Distinctively, the TT unit of chromophore **b** showed electro-negativity first and transferred to electro-positivity with increasing solvent dielectric constant (Table S1′–S6′, ESI†). This was in relation to the strong electron-withdrawing ability of the TCF acceptor and the strong electron delocalization ability of the TT unit. Furthermore, the charge difference of each unit for a given chromophore molecule tends to decrease with the increase of the solvent polarity, suggesting that increasing the solvent polarity could stabilize the charge separation. Therefore, the study of the molecular electron structure is a guideline for the chromophore design to tune the quadratic NLO properties.

Bond-length alternation. The bond length alternation (BLA) was reported as a key structural parameter that can be correlated with the ground state geometry of the molecule and hyperpolarizability.[25] BLA was defined as the average difference in length between adjacent carbon–carbon single and double bonds in the molecule. Based on the two-state model,[58] there is an optimal structure about the combination of each unit of the chromophore.[25] As reported previously, the semiempirical calculations were mainly performed on the push–pull polyene chromophores, while few studies were performed on the heteroaromatic ring based chromophores. For polyene chromophores, tuning the suitable combination of a donor and a acceptor as well as the π-bridge can optimize the BLA and β. It showed that the maximum β value can be achieved when the BLA values are intermediate ($\pm 0.05 \pm 0.01$ Å). Consequently, the BLA values of the π-bridges can be regarded as a measure of ground-state polarization and as an important parameter for NLO response.

For the heteroaromatic ring based chromophores (**a–d**) and two polyene chromophores (**e** and **f**), as shown in Fig. 5(a), the BLA of six chromophores in the gas phase and six solvents was calculated (Table S1–S6, ESI†) to study the solvent dependence of BLA and the correlation between β_{tot} and BLA. For chromophore **d** with combined bridges, the BLA is between −0.04 Å and −0.05 Å and it also shows the largest β_{tot}, which is in consistent with the BLA model. For chromophore **b** with a single TT bridge, the absolute value of BLA shows the minimum value but the β_{tot} is as large as that of chromophore **d**. We speculated that chromophores using the TT unit as the π-bridge were not suitable for this BLA model. Moreover, all the chromophores showed a similar decaying trend in BLA with an increase of solvent polarity. As the solvent polarity increased, the occupancy of zwitterionic form arose to the even distribution of the two resonance forms. The BLA of chromophore **d** demonstrated that it had a larger β_{tot} value than that of other chromophores according to the BLA model proposed by Marder *et al.*[59]

Energy gaps (ΔE). The ΔE between HOMO and LUMO of six chromophores was calculated in a vacuum and six different solvents. As shown in Fig. 5(b), the ΔE of all the chromophores displayed a similar decaying trend as a function of the increasing solvent polarity. Thus, the solvent-dependent behaviors of all the chromophores studied here suggested that increasing the solvent dielectric constant could reduce the ΔE of the chromophore molecules and tend to favor ICT. Moreover, the ΔE results calculated by the DFT method were in consistent with the experimental results using the CV method and the spectral analysis. It also demonstrated that this calculated method can be a good alternative to predict ΔE.

Frontier molecular orbitals. Frontier molecular orbitals (FMOs) of chromophores **a–f** were calculated to show the relationship between the structures and properties. As shown in Fig. 6, for all the chromophores, the HOMOs were delocalized on the julolidinyl-based donors and π-bridges while the LUMOs were localized in the conjugated bridges and concentrated on the acceptors. The results indicated that increasing the length of the π-bridges allowed an efficient ICT from the donor to the acceptor. Moreover, for chromophore **a**, the optimized

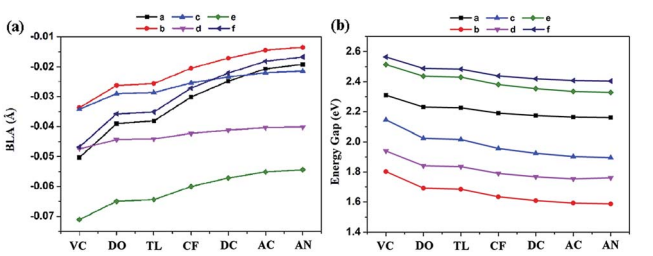

Fig. 5 The calculated (a) BLA and (b) energy gap values of chromophores **a–f** in a vacuum and six different solvents.

 This journal is © The Royal Society of Chemistry 2015

Published on 24 September 2014. Downloaded by Michigan State University on 26/01/2016 23:56:33.

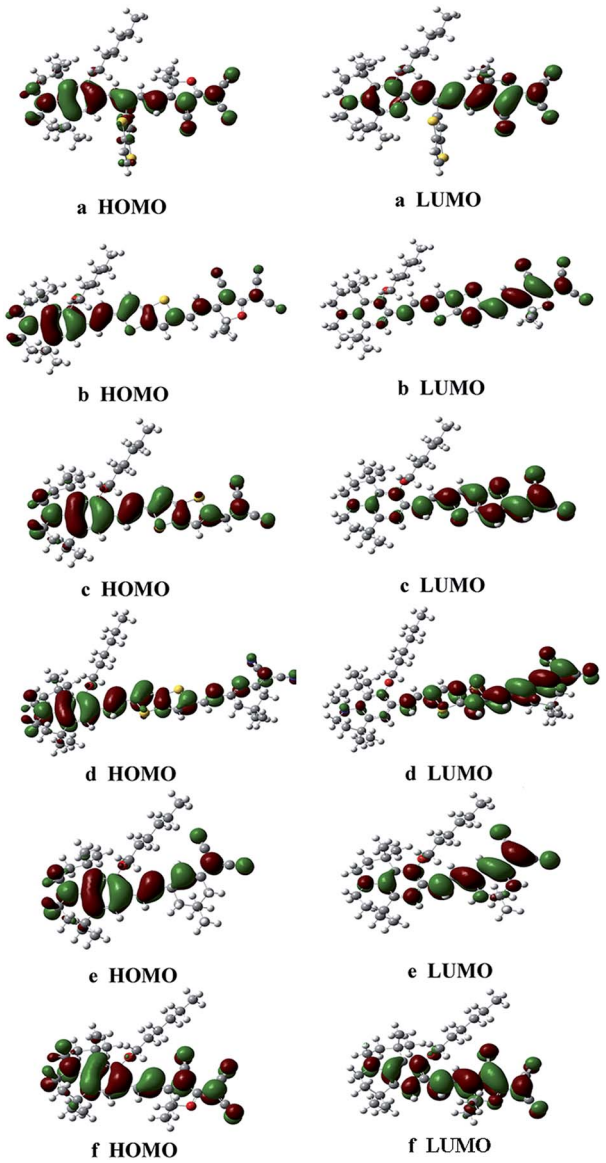

Fig. 6 The HOMO and LUMO frontier molecular orbitals of chromophores **a**–**f**.

perpendicular spatial configuration of the TT unit disfavored the ICT on the main axis. It was worth highlighting that the TT unit contributed roughly equal to both HOMOs and LUMOs of chromophore **b**, which promoted the ICT. Thus, chromophores with longer π-bridges and stronger acceptors were supposed with lower ΔE, which was in accord with the experimental results.

EO properties

According to the experimental and calculated results of chromophores **a**–**f** mentioned above, chromophores **a** and **b** were chosen to evaluate the EO activity for such reasons. Firstly, both of them showed good thermal stability. Secondly, chromophore **b** exhibited the largest β_{tot} and $\mu\beta_{tot}$ values according to the DFT calculations. Then, they both showed good photophysical properties. Finally, the influence of the TT unit as the lateral moiety or π-bridge of the chromophore could be studied. Thus, amorphous polycarbonate (APC) guest–host polymer films incorporating 20 wt% of chromophores **a** and **b** were prepared. Both EO polymers showed a similar T_g around 140 °C and the poling temperature was about 5 °C higher than T_g. Another two critical parameters determining the r_{33} values were poling voltage and time. The optimum condition was poled at 145 °C for 18 min under the electric field of 11.5 kV. After that, the films were cooled to room temperature rapidly followed by the removal of the poling voltage. A thick film of aluminium (around 100 nm) was sputtered on the poled films, and then the EO coefficients of them were measured by the Teng–Man method at a wavelength of 1.31 μm. The maximum r_{33} value of 94 pm V^{-1} for chromophore **a** was achieved. However, chromophore **b** did not show the large r_{33} value because of the poor compatibility in APC films. Then, 10 wt% of the chromophore **b** was doped into APC to make the guest–host polymer film follow the same abovementioned procedures. The optimum condition was poled at 155 °C for 25 min under the electric field of 11 kV. The maximum r_{33} value was only around 20 pm V^{-1}. Chromophore **b** was calculated with the largest μ and β_{tot} values, however, these values and the good planarity also make it easy to form the antiparallel aggregation, leading to the sharply attenuated r_{33} value. As to chromophore **a**, the TT unit in this molecule affected both the steric effect and the electron effect, resulting in the decreased intermolecular dipole–dipole interactions. We speculated that the steric effect could play a major role in the macroscopic NLO properties, while the electron effect could play a crucial role in the microscopic NLO properties.

Photochemical stability

To investigate the photochemical stability of chromophores **a** and **b**, they were separately dissolved in chloroform solutions (5×10^{-5} M), and then irradiated with 450 nm light for an hour. As shown in Fig. 7(a) and (b), after irradiation, the UV-Vis-NIR absorption spectra of chromophore **b** dropped more extensively than that of chromophore **a**. It also demonstrated that chromophore **a** showed better photostability and EO properties than those of chromophore **b**. This might be attributed to the lower ΔE of chromophore **b** (0.85 eV) than that of chromophore **a**

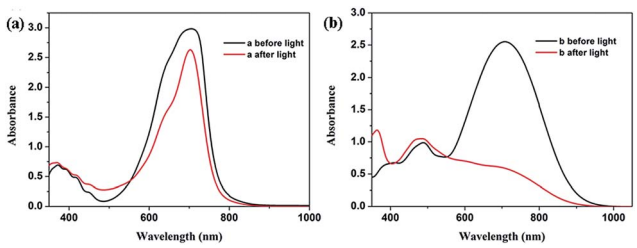

Fig. 7 The UV-Vis-NIR absorption spectra of the solutions were irradiated with 450 nm light. The spectra before and after irradiation with 450 nm light of $CHCl_3$ solutions for chromophore **a** (a) and chromophore **b** (b).

Published on 24 September 2014. Downloaded by Michigan State University on 26/01/2016 23:56:33.

(1.11 eV), which made chromophore **b** more sensitive to light and oxygen than chromophore **a**. This was in consistent with the experimental and calculated ΔE results, which showed that chromophore **b** had lower ΔE than chromophore **a**. Consequently, for chromophores with large microscopic NLO properties as **b**, how to improve the poling efficiency and solubility and photochemical stability in host polymer films and efficiently translate the high microscopic NLO properties to macroscopic r_{33} values is an urgent challenge. Such as optimizing the structure by introducing the bulk groups into the donor or acceptor part was an alternative under study.

Conclusions

A series of julolidinyl-based chromophores based on different types of π-bridges, including the TT unit and the isophorone unit, and TCF or dicyanomethylene acceptors, have been synthesized and investigated. The structure–property relationship of the studied chromophores was explored using experimental and calculated data. Electrochemical and solvatochromic behaviour analyses as well as DFT calculations were also carried out to show the microscopic NLO properties of the chromophores. Chromophore **b** displayed a larger $\mu\beta_{tot}$ value and narrower energy gap than those of chromophore **a**, whereas its r_{33} value was almost three times smaller with respect to that of chromophore **a**. This might be attributed to the better photochemical stability and the steric structure of the TT unit of chromophore **a**, leading to the increased poling efficiency. Chromophore **d** with a combination of TT unit and isophorone unit as the π-bridge was calculated as the D–A–π–A structure. It preferred to display the blue-shifted phenomenon of ICT absorption and high microscopic NLO properties that helped to overcome the nonlinearity–transparency trade-off. However, this new 'mismatched' combination of the π-bridge made chromophore **d** display the sharply decreased thermal stability and weak low-energy absorption because of the inefficient ICT. Thus, searching for the 'matched' combination of π-bridges with good thermal stability is a big challenge. Moreover, good thermal stability and NLO properties made chromophores **a** and **b** have great potential for new generation organic EO devices. Thus, the improvement of translating the large β value into bulk EO activity of materials is a big challenge we need to overcome in the near future.

Acknowledgements

We are grateful to the National Natural Science Foundation of China (nos 11104284, 21003143 and 61101054) for financial support. All calculations were performed on the cluster of Key Laboratory of Theoretical and Computational Photochemistry, Ministry of Education, China.

Notes and references

1 R. L. Gieseking, S. Mukhopadhyay, C. Risko, S. R. Marder and J.-L. Brédas, *Adv. Mater.*, 2014, **26**, 68–84.
2 L. R. Dalton, P. A. Sullivan, D. H. Bale and B. C. Olbricht, *Solid-State Electron.*, 2007, **51**, 1263–1277.
3 C. R. Moylan, R. J. Twieg, V. Y. Lee, S. A. Swanson, K. M. Betterton and R. D. Miller, *J. Am. Chem. Soc.*, 1993, **115**, 12599–12600.
4 C. Zhang, A. S. Ren, F. Wang, J. Zhu, L. R. Dalton, J. N. Woodford and C. H. Wang, *Chem. Mater.*, 1999, **11**, 1966–1968.
5 P. Kaur, M. Kaur, G. Depotter, S. Van Cleuvenbergen, I. Asselberghs, K. Clays and K. Singh, *J. Mater. Chem.*, 2012, **22**, 10597–10608.
6 J. Luo, X.-H. Zhou and A. K. Y. Jen, *J. Mater. Chem.*, 2009, **19**, 7410–7424.
7 D. L. Elder, S. J. Benight, J. Song, B. H. Robinson and L. R. Dalton, *Chem. Mater.*, 2014, **26**, 872–874.
8 G. Jayamurugan, O. Dumele, J.-P. Gisselbrecht, C. Boudon, W. B. Schweizer, B. Bernet and F. Diederich, *J. Am. Chem. Soc.*, 2013, **135**, 3599–3606.
9 J. Gao, Y. Cui, J. Yu, Z. Wang, M. Wang, J. Qiu and G. Qian, *Macromolecules*, 2009, **42**, 2198–2203.
10 W. C. W. Leu and C. S. Hartley, *Org. Lett.*, 2013, **15**, 3762–3765.
11 S.-i. Kato and F. Diederich, *Chem. Commun.*, 2010, **46**, 1994–2006.
12 G. Yu, X. Zhao, M. Niu, X. Huang, H. Zhang and W. Chen, *J. Mater. Chem. C*, 2013, **1**, 3833–3841.
13 L. Dalton, W. Steier and B. Robinson, *J. Mater. Chem.*, 1999, **9**, 1905–1920.
14 Y. Liao, S. Bhattacharjee, K. A. Firestone, B. E. Eichinger, R. Paranji, C. A. Anderson, B. H. Robinson, P. J. Reid and L. R. Dalton, *J. Am. Chem. Soc.*, 2006, **128**, 6847–6853.
15 X. Liu, Y. Sun, L. A. Perez, W. Wen, M. F. Toney, A. J. Heeger and G. C. Bazan, *J. Am. Chem. Soc.*, 2012, **134**, 20609–20612.
16 T. Inouchi, T. Nakashima and T. Kawai, *J. Phys. Chem. A*, 2014, **118**, 2591–2598.
17 K. Y. Suponitsky, Y. Liao and A. m. E. Masunov, *J. Phys. Chem. A*, 2009, **113**, 10994–11001.
18 S. Achelle, A. Barsella, C. Baudequin, B. Caro and F. Robin-le Guen, *J. Org. Chem.*, 2012, **77**, 4087–4096.
19 J. Wu, B. A. Wilson, D. W. Smith Jr and S. O. Nielsen, *J. Mater. Chem. C*, 2014, **2**, 2591–2599.
20 G. S. He, J. Zhu, A. Baev, M. Samoć, D. L. Frattarelli, N. Watanabe, A. Facchetti, H. Ågren, T. J. Marks and P. N. Prasad, *J. Am. Chem. Soc.*, 2011, **133**, 6675–6680.
21 H. Meier, *Angew. Chem., Int. Ed.*, 2005, **44**, 2482–2506.
22 G. Yu, X. Zhao, M. Niu, X. Huang, H. Zhang and W. Chen, *J. Mater. Chem. C*, 2013, **1**, 3833–3841.
23 B. S. Ault and G. C. Pimentel, *J. Phys. Chem.*, 1975, **79**, 621–626.
24 C. Botta, E. Cariati, G. Cavallo, V. Dichiarante, A. Forni, P. Metrangolo, T. Pilati, G. Resnati, S. Righetto, G. Terraneo and E. Tordin, *J. Mater. Chem. C*, 2014, **2**, 5275–5279.
25 M. Blanchard-Desce, V. Alain, P. V. Bedworth, S. R. Marder, A. Fort, C. Runser, M. Barzoukas, S. Lebus and R. Wortmann, *Chem.–Eur. J.*, 1997, **3**, 1091–1104.

 This journal is © The Royal Society of Chemistry 2015

Published on 24 September 2014. Downloaded by Michigan State University on 26/01/2016 23:56:33.

26 X.-H. Zhou, J. Luo, J. A. Davies, S. Huang and A. K. Y. Jen, *J. Mater. Chem.*, 2012, **22**, 16390–16398.
27 H. Choi, J. K. Lee, K. H. Song, K. Song, S. O. Kang and J. Ko, *Tetrahedron*, 2007, **63**, 1553–1559.
28 G. Wu, F. Kong, J. Li, W. Chen, C. Zhang, Q. Chen, X. Zhang and S. Dai, *Synth. Met.*, 2013, **180**, 9–15.
29 G. Wu, F. Kong, J. Li, X. Fang, Y. Li, S. Dai, Q. Chen and X. Zhang, *J. Power Sources*, 2013, **243**, 131–137.
30 J. Wu, C. Peng, H. Xiao, S. Bo, L. Qiu, Z. Zhen and X. Liu, *Dyes Pigm.*, 2014, **104**, 15–23.
31 J. Wu, S. Bo, J. Liu, T. Zhou, H. Xiao, L. Qiu, Z. Zhen and X. Liu, *Chem. Commun.*, 2012, **48**, 9637–9639.
32 Y. Ji, Y. Qian and W. Lu, *J. Mater. Chem.*, 2012, **22**, 12375–12380.
33 X. Ma, F. Ma, Z. Zhao, N. Song and J. Zhang, *J. Mater. Chem.*, 2010, **20**, 2369–2380.
34 S. R. Marder, D. N. Beratan and L.-T. Cheng, *Science*, 1991, **252**, 103–106.
35 M. C. Ruiz Delgado, V. Hernández, J. Casado, J. T. López Navarrete, J.-M. Raimundo, P. Blanchard and J. Roncali, *Chem.–Eur. J.*, 2003, **9**, 3670–3682.
36 J.-M. Raimundo, P. Blanchard, N. Gallego-Planas, N. Mercier, I. Ledoux-Rak, R. Hierle and J. Roncali, *J. Org. Chem.*, 2002, **67**, 205–218.
37 G. Prampolini, F. Bellina, M. Biczysko, C. Cappelli, L. Carta, M. Lessi, A. Pucci, G. Ruggeri and V. Barone, *Chem.–Eur. J.*, 2013, **19**, 1996–2004.
38 B. Milián, E. Ortí, V. Hernández, J. T. López Navarrete and T. Otsubo, *J. Phys. Chem. B*, 2003, **107**, 12175–12183.
39 J. Casado, V. Hernández, O. K. Kim, J. M. Lehn, J. T. López Navarrete, S. Delgado Ledesma, R. Ponce Ortiz, M. C. Ruiz Delgado, Y. Vida and E. Pérez-Inestrosa, *Chem.–Eur. J.*, 2004, **10**, 3805–3816.
40 O.-K. Kim, A. Fort, M. Barzoukas, M. Blanchard-Desce and J.-M. Lehn, *J. Mater. Chem.*, 1999, **9**, 2227–2232.
41 O.-K. Kim and J.-M. Lehn, *Chem. Phys. Lett.*, 1996, **255**, 147–150.
42 A. B. Marco, R. Andreu, S. Franco, J. Garin, J. Orduna, B. Villacampa, B. E. Diosdado, J. T. Lopez Navarrete and J. Casado, *Org. Biomol. Chem.*, 2013, **11**, 6338–6349.
43 V. P. Rao, K. Y. Wong, A. K.-Y. Jen and K. J. Drost, *Chem. Mater.*, 1994, **6**, 2210–2212.
44 H. Bronstein, E. Collado-Fregoso, A. Hadipour, Y. W. Soon, Z. Huang, S. D. Dimitrov, R. S. Ashraf, B. P. Rand, S. E. Watkins, P. S. Tuladhar, I. Meager, J. R. Durrant and I. McCulloch, *Adv. Funct. Mater.*, 2013, **23**, 5647–5654.
45 I. Meager, R. S. Ashraf, S. Rossbauer, H. Bronstein, J. E. Donaghey, J. Marshall, B. C. Schroeder, M. Heeney, T. D. Anthopoulos and I. McCulloch, *Macromolecules*, 2013, **46**, 5961–5967.
46 S. Tang and J. Zhang, *J. Comput. Chem.*, 2012, **33**, 1353–1363.
47 P. Boldt, G. Bourhill, C. Bräuchle, Y. Jim, R. Kammler, C. Müller, J. Rase and J. Wichern, *Chem. Commun.*, 1996, 793–795.
48 A. B. Marco, R. Andreu, S. Franco, J. Garín, J. Orduna, B. Villacampa and R. Alicante, *Tetrahedron*, 2013, **69**, 3919–3926.
49 J. L. Oudar and D. S. Chemla, *J. Chem. Phys.*, 1977, **66**, 2664–2668.
50 J. Luo, J. Hua, J. Qin, J. Cheng, Y. Shen, Z. Lu, P. Wang and C. Ye, *Chem. Commun.*, 2001, 171–172.
51 J. Hua, J. Luo, J. Qin, Y. Shen, Y. Zhang and Z. Lu, *J. Mater. Chem.*, 2002, **12**, 863–867.
52 C. Teng and H. Man, *Appl. Phys. Lett.*, 1990, **56**, 1734–1736.
53 S. Liu, M. A. Haller, H. Ma, L. R. Dalton, S. H. Jang and A. Y. Jen, *Adv. Mater.*, 2003, **15**, 603–607.
54 M. He, T. M. Leslie and J. A. Sinicropi, *Chem. Mater.*, 2002, **14**, 4662–4668.
55 D. H. Park, C. H. Lee and W. N. Herman, *Opt. Express*, 2006, **14**, 8866–8884.
56 X.-H. Zhou, J. Davies, S. Huang, J. Luo, Z. Shi, B. Polishak, Y.-J. Cheng, T.-D. Kim, L. Johnson and A. Jen, *J. Mater. Chem.*, 2011, **21**, 4437–4444.
57 X. Wang, S. Chen, Y. Sun, M. Zhang, Y. Li, X. Li and H. Wang, *Polym. Chem.*, 2011, **2**, 2872–2877.
58 M. Barzoukas, C. Runser, A. Fort and M. Blanchard-Desce, *Chem. Phys. Lett.*, 1996, **257**, 531–537.
59 S. R. Marder, J. W. Perry, B. G. Tiemann, C. B. Gorman, S. Gilmour, S. L. Biddle and G. Bourhill, *J. Am. Chem. Soc.*, 1993, **115**, 2524–2526.
60 M. J. Frisch, G. W. Trucks, H. B. Schlegel, G. E. Scuseria, M. A. Robb, J. R. Cheeseman, J. A. Montgomery Jr, T. Vreven, K. Kudin and J. C. Burant, *et al.*, *Gaussian 09, Revision A.02*, Gaussian, Inc., Wallingford CT, 2009.